

Cavitation Inception and Dynamics in Vortical Flows

Steve L. Ceccio

*Mechanical Engineering
Naval Architecture & Marine Engineering*

University of Michigan
Ann Arbor, MI, 48109

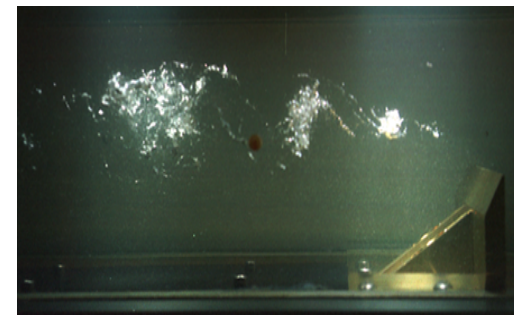
***American Physical Society
62nd Annual Meeting
Division of Fluid Dynamics***

University of
MICHIGAN



Vortex Cavitation

- **Regions of concentrated vorticity can form in many flows:**
 - *Tip Vortices*
 - *Leakage Vortices*
 - *Wake Vortices*
 - *Turbulent Shear Flows*
- **The pressure in the core of the vortex is lower than that of the surrounding fluid.**
- **Small bubbles (nuclei) in the core of the vortex grow when exposed to the low pressure.**



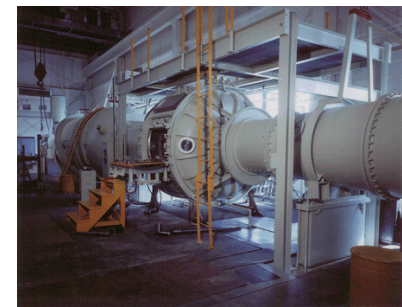
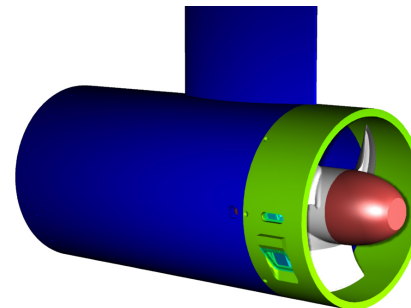
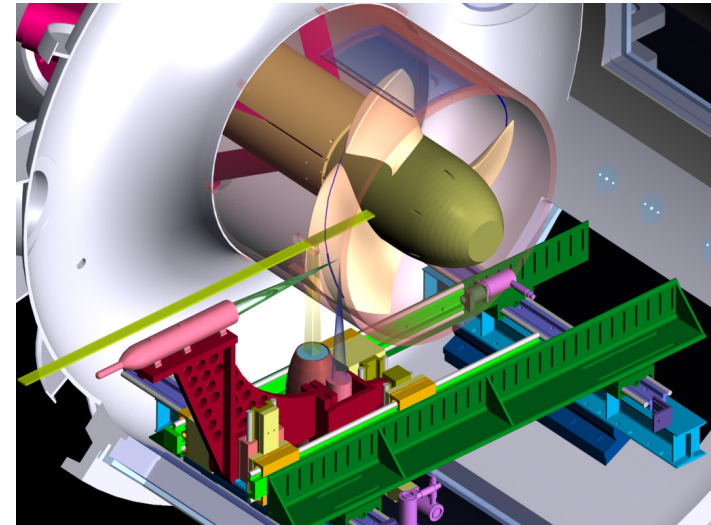
Reviewed by Arndt (2002), Annual Reviews of Fluid Mechanics

Vortex Cavitation in Turbomachinery

Issue: Incipient Tip Leakage Cavitation can be detected acoustically well before visual inception on ducted rotors.

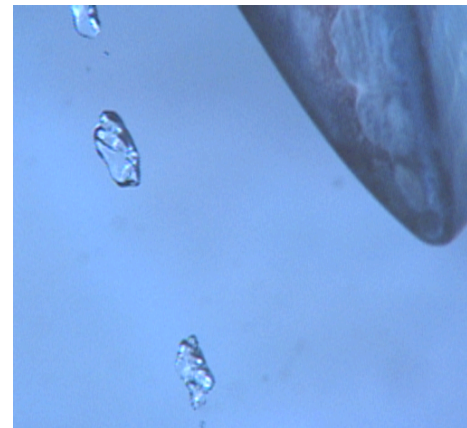
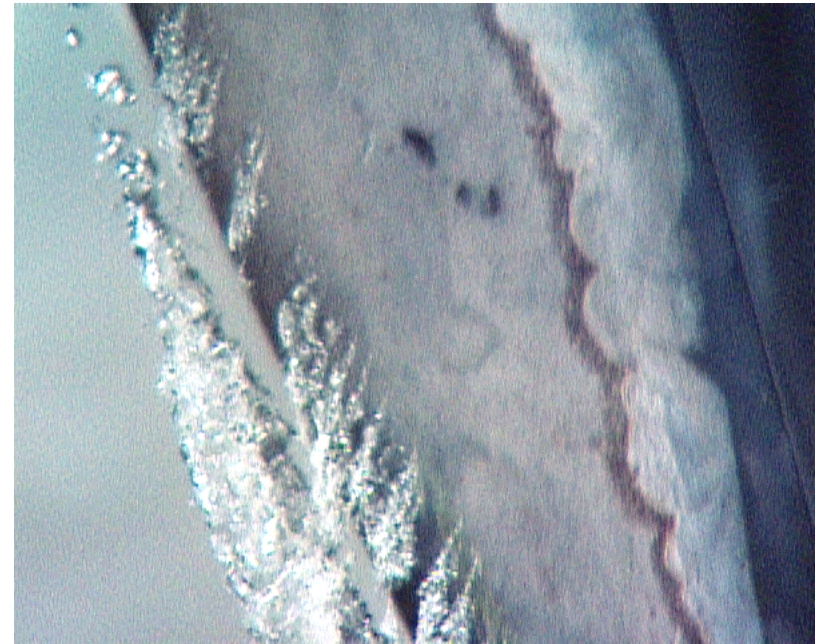
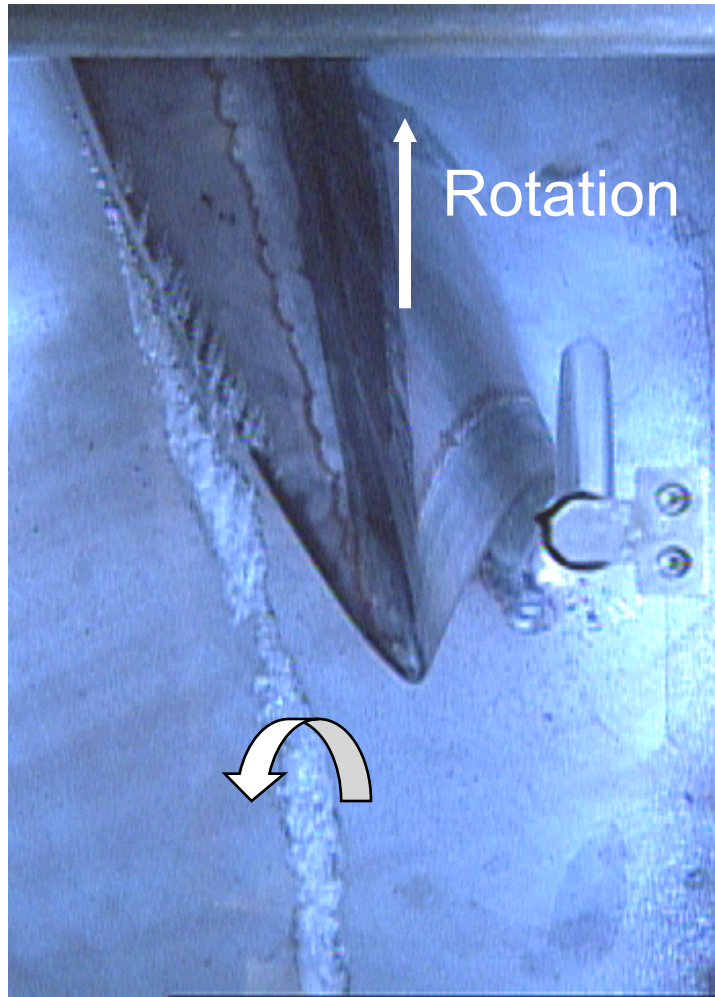
Issue: TLC Inception occurs at higher than expected cavitation numbers.

Objective: Understand the *physical processes* leading to TLV inception by studying a canonical open and ducted rotors up to 1 meter in diameter.

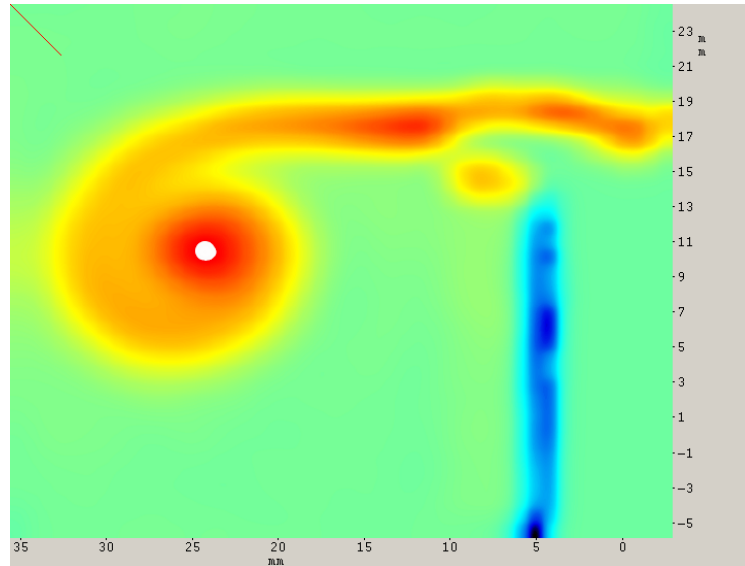


NSWC-CD 36" Water Tunnel

Tip Leakage Cavitation

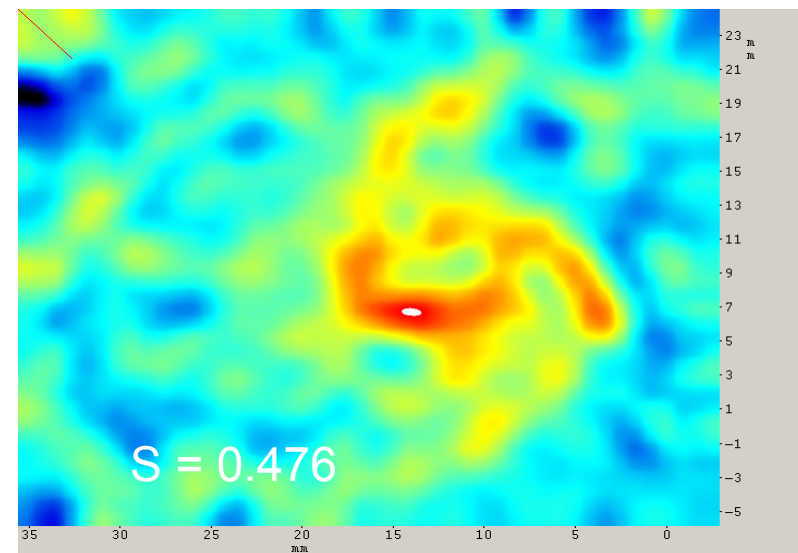
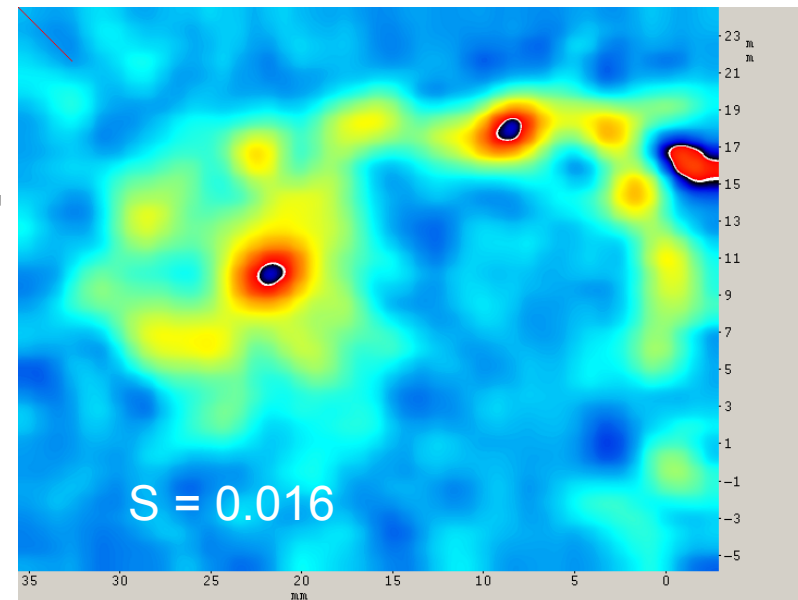


PIV Measurements of Vortical Flow In Tip Leakage Region



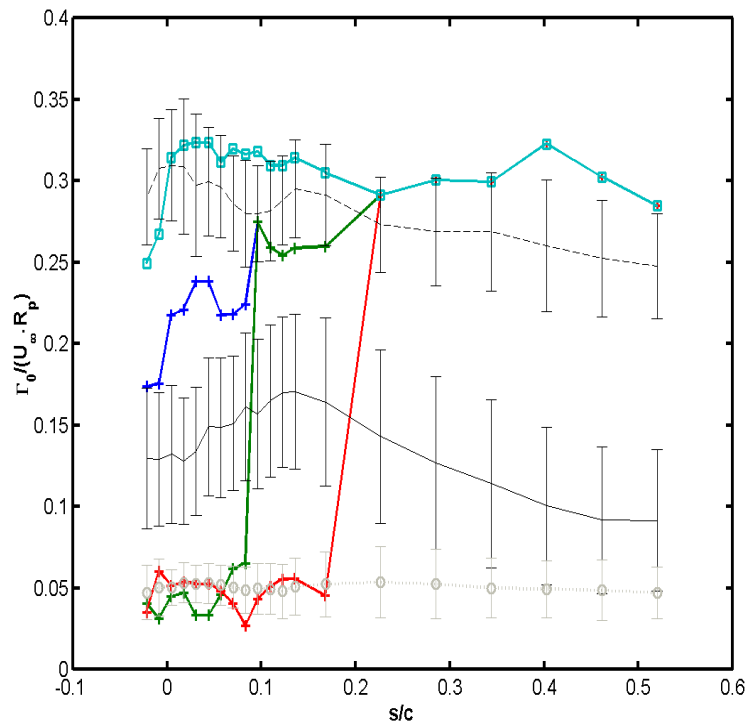
**Identification of High Vorticity Regions
Can Be Lost Through Phase Averaging**

*Oweis, Fry, Chesnakas, Jessup, and
Ceccio, JFE, (2005a) (2005b)*



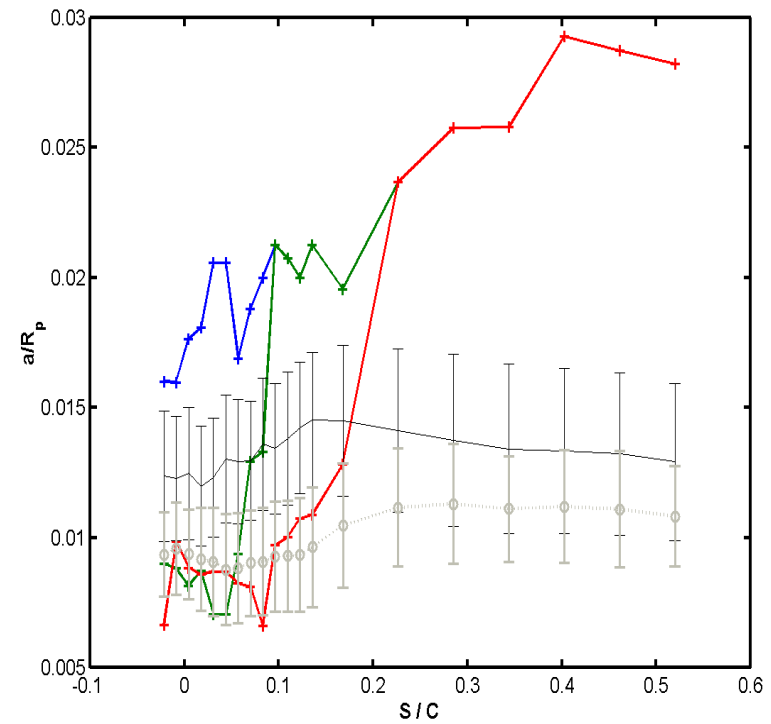
Identification of High Vorticity Regions Can Be Lost Through Phase Averaging

PIV reveals time variation in vortex patterns, spatial positions, and properties
Oweis and Ceccio. EIF. (2005).



Circulation

438 RPM



Core radius

Sometimes TLV Cavitation Made a “Popping” or “Chirping” Sound

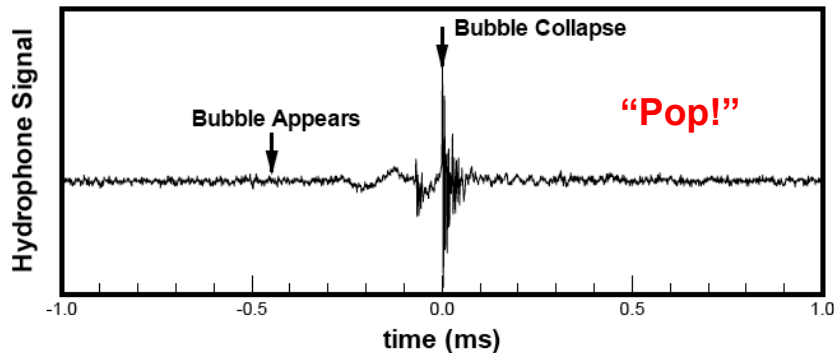


Figure 7. Acoustic signal from a single bubble (pop).

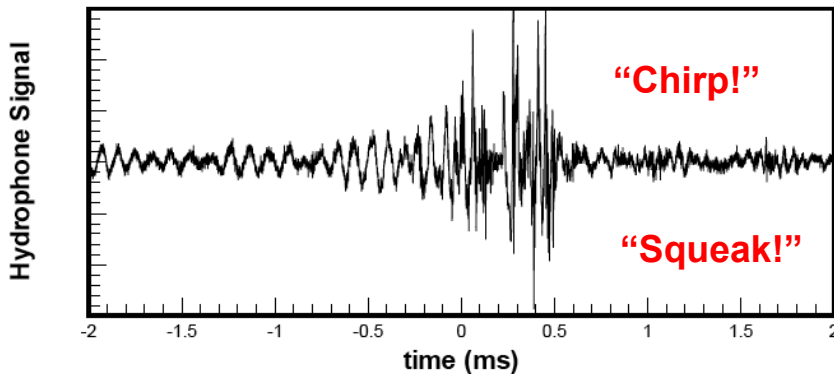
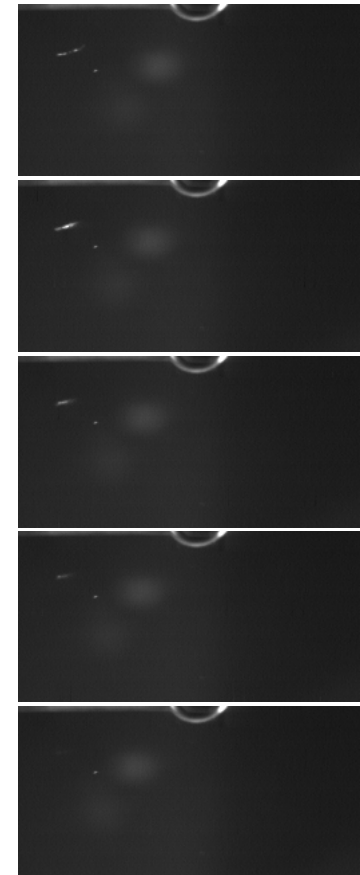
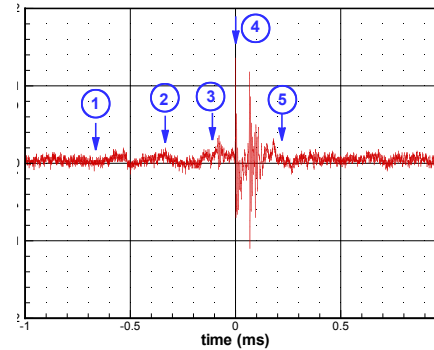


Figure 8. Acoustic signal from a bubble trail (chirp).



*Incipient TLV cavitation and an accompanying noise signal.
(Chesnakas and Jessup, Proc. ASME, 2003)*

Prediction of Inception Pressure and Location is Difficult

Measured Vortex Core Properties:

- Instantaneous circulations, Γ_O , and core sizes, a , are measured.
- The typical (average) pressure drop in the core is determined:

$$\Delta P = p_C - p_\infty = -\eta_3 \rho_f \left(\frac{\Gamma_O}{2\pi a} \right)^2$$

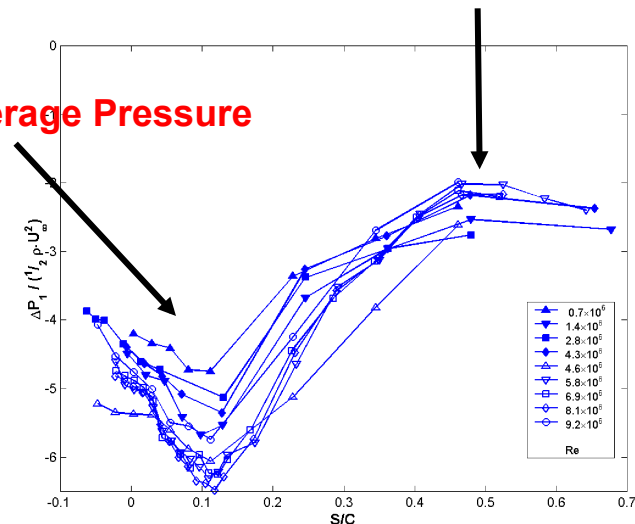
- Pressure coefficient is determined as a function of downstream distance, s/c .

Unexpected Findings

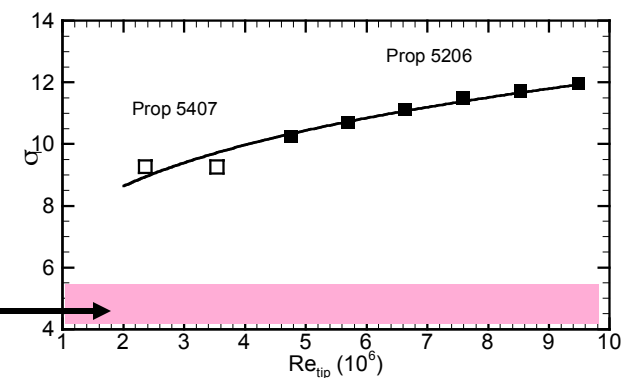
- Inception occurred **downstream** of the minimum mean pressure location on the 5206 and 5407 rotors.
- Inception occurs at much **higher pressures**.
- Inception controlled by **unsteady pressures**.

Location of SVC Inception

Minimum Average Pressure



Range of $-C_p$
at $s/c \sim 0.5$

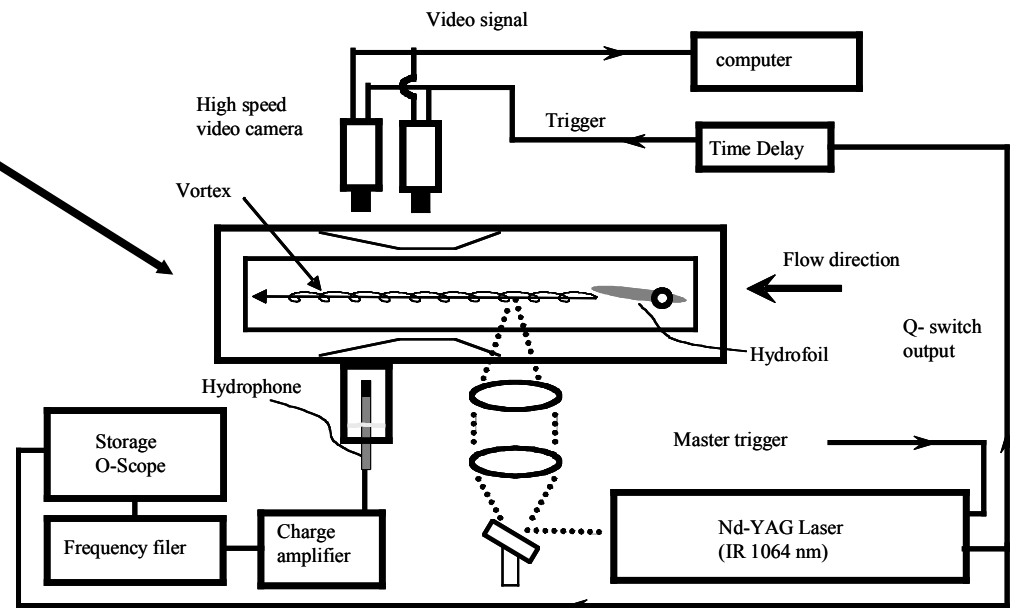


Basic Experiments Were Conducted to Address Basic TVC Flows

- How are **nuclei** captured by the vortex?
- What causes the **core pressure** of the cavitating vortex to be suddenly reduced? (Merging, stretching, axial core jet/wakes in the vortex?)
- How does the TVC bubble make **noise**? (Is noise produced during growth, convection, and/or collapse?)

Choi and Ceccio, JFM, (2007)

Vortex Cavitation Bubbles in a Single Vortex



9- Inch Cavitation Tunnel at the University of Michigan

Inlet Vortex Properties for Four Conditions

	$\alpha=4^\circ$ (1)		$\alpha=4.5^\circ$ (2)	
	Γ_O , m ² /s	r_C , mm	Γ_O , m ² /s	r_C , mm
Foil With Trip (T)	0.252 +/-0.015	4.76 +/-0.31	0.288 +/-0.018	5.15 +/-0.35
Foil Without Trip (T)	0.257 +/-0.013	3.75 +/-0.20	0.302 +/-0.015	4.20 +/-0.23

***SPIV Measurements of Mean Flow.
Axial jet/wake in the vortex core was not present.***

Gaussian Vortex With Axial Jet

$$u_{\theta}(r) = \frac{\Gamma_o}{2\pi r} (1 - e^{-\alpha(r/r_c)^2})$$

Tangential Velocity

$$u_{\theta}(r_c) = \beta \frac{\Gamma_o}{2\pi r_c}$$

Maximum Tangential Velocity ($\beta = 0.715$)

$$P(r) - P_{\infty} = \int_{\infty}^0 -\frac{\rho u_{\theta}^2(r)}{r} dr = -\rho \left(\frac{\Gamma_o}{2\pi r_c} \right)^2 \left(\frac{1}{2(r/r_c)^2} \right) \times \begin{bmatrix} -1 + 2e^{-\alpha(r/r_c)^2} - e^{-2\alpha(r/r_c)^2} \\ -2\alpha(r/r_c)^2 Ei(\alpha(r/r_c)^2) \\ +2\alpha(r/r_c)^2 Ei(2\alpha(r/r_c)^2) \end{bmatrix}$$

Radial Pressure Distribution

$$P_c = P_{\infty} - \eta \rho \left(\frac{\Gamma_o}{2\pi r_c} \right)^2$$

Minimum Core Pressure ($\eta = 0.870$)

$$\sigma_{\infty} = (P_{\infty} - P_V) / \frac{1}{2} \rho U_{\infty}^2$$

Cavitation Number

$$\sigma_c = -\frac{2\eta}{\beta^2} + \left(\frac{2\pi r_c U_{\infty}}{\beta \Gamma_o} \right)^2 \left[1 - \left(\frac{U_c}{U_{\infty}} \right)^2 + \sigma_{\infty} \right]$$

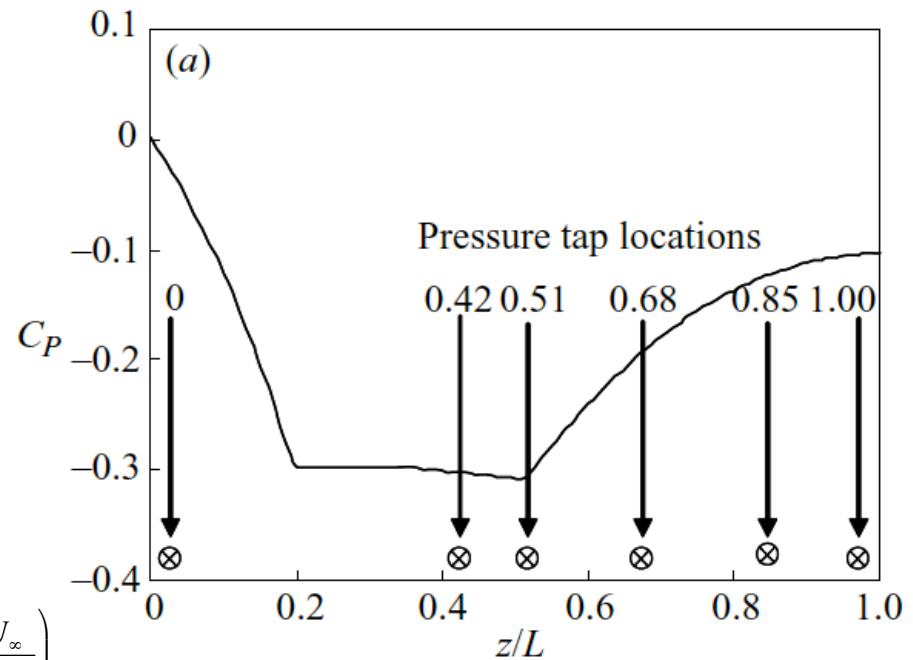
Cavitation Number on Vortex Axis

Vortex Is passed Through a Venturi to Lower and Recover Surrounding Static Pressure

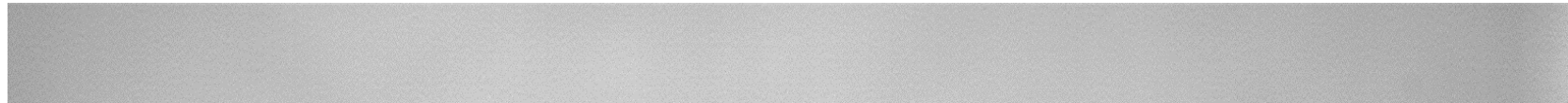
- Measured pressure along the Venturi with 6 pressure taps.
- Pressures used to estimate the loss coefficients for the throat, straight passage, and diffuser.
- The vortex core axial velocity estimated using relation derived by Darmfil *et al.* (2001).

$$\frac{\Omega_\infty^2}{a(z)/A_\infty} - \left(\frac{1}{a(z)/A_\infty} \right)^2 + \left(\frac{U_\infty/U_{C,\infty}(1 - a_\infty/A_\infty)}{A(z)/A_\infty - a(z)/A_\infty} \right)^2 = \Omega_\infty^2 - 1 + \left(\frac{U_\infty}{U_{C,\infty}} \right)^2$$

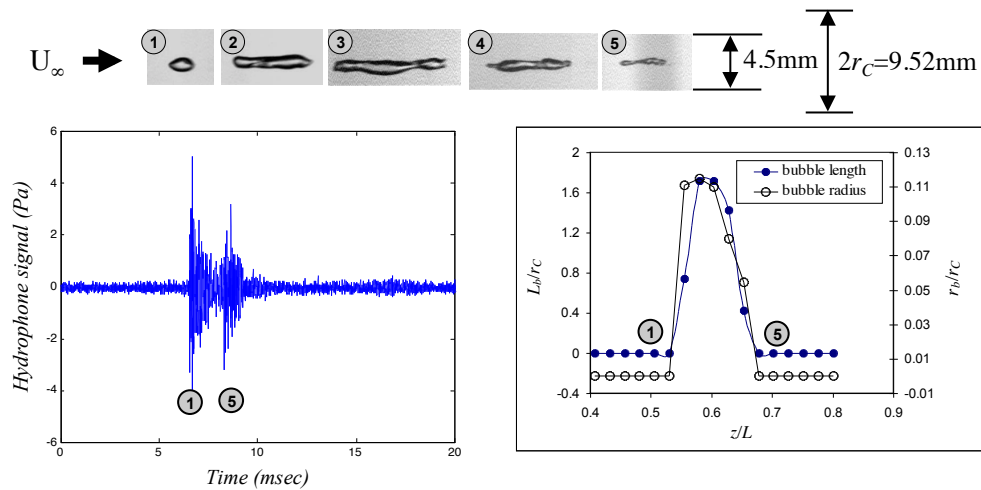
- **The vortex core pressure is then computed.**



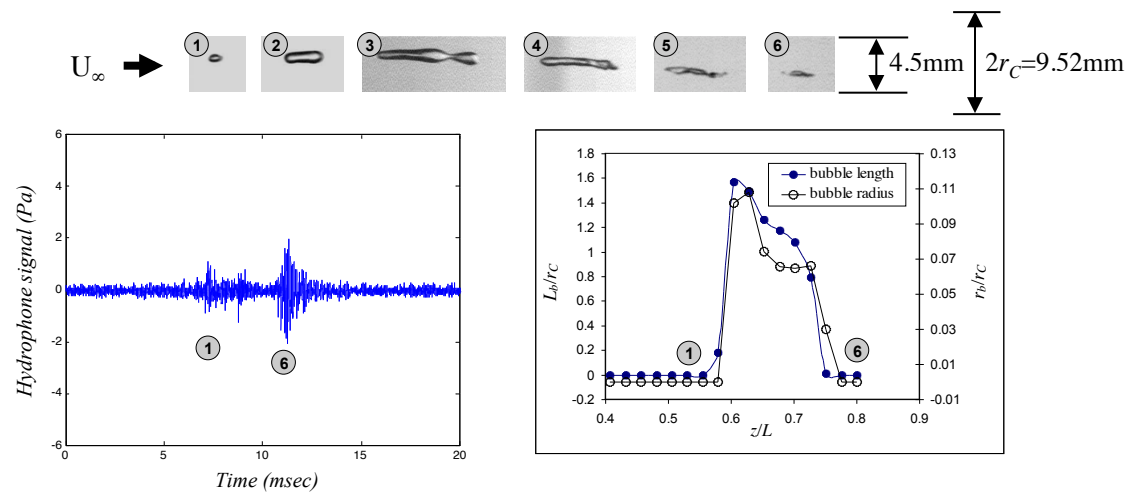
$$C_p = (P_c(z) - P_\infty) / (\rho(\beta\Gamma_c / (2\pi r_c))^2 / 2)$$



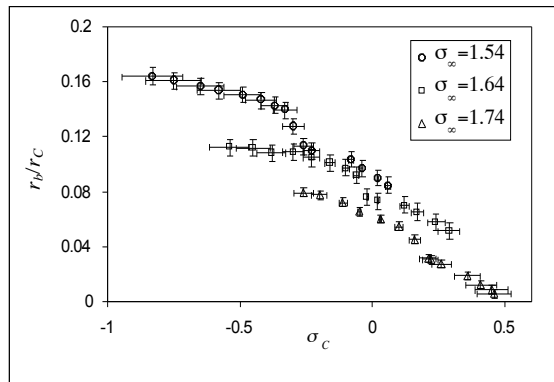
Time Series of Individual Cavitation Bubbles



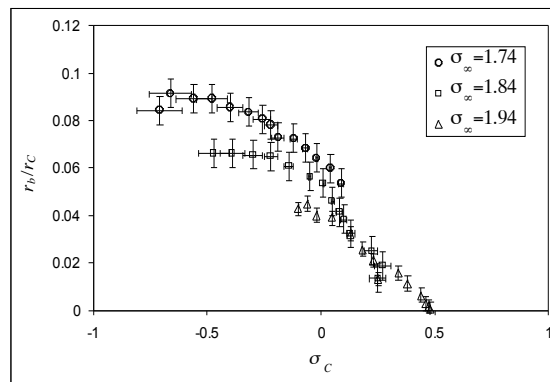
T1



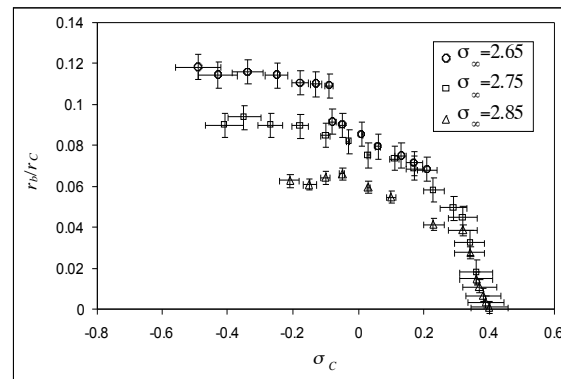
Elongated Bubble Radius versus σ_c



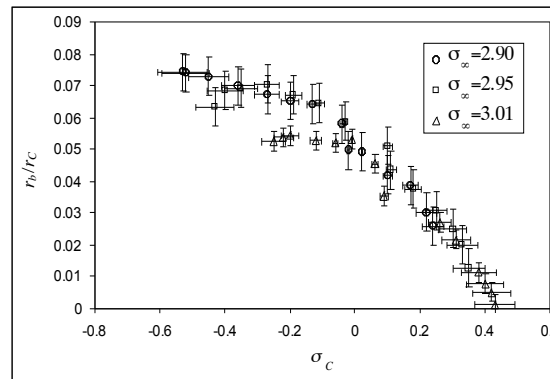
(a) T1



(b) T2



(c) R1



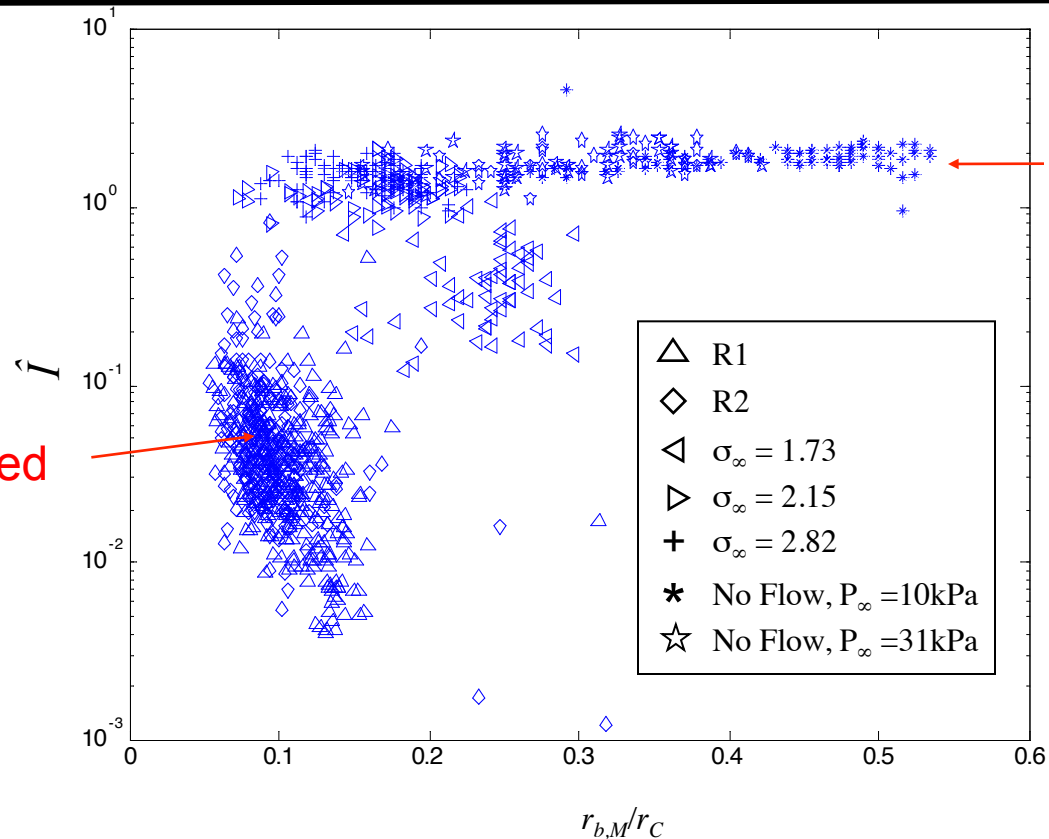
(d) R2

Results are very sensitive to small variations in vortex properties.

Acoustic Impulse of Collapse versus Equivalent Radius

$$P_A \sim \frac{\partial^2 Q}{\partial t^2}$$

Elongated



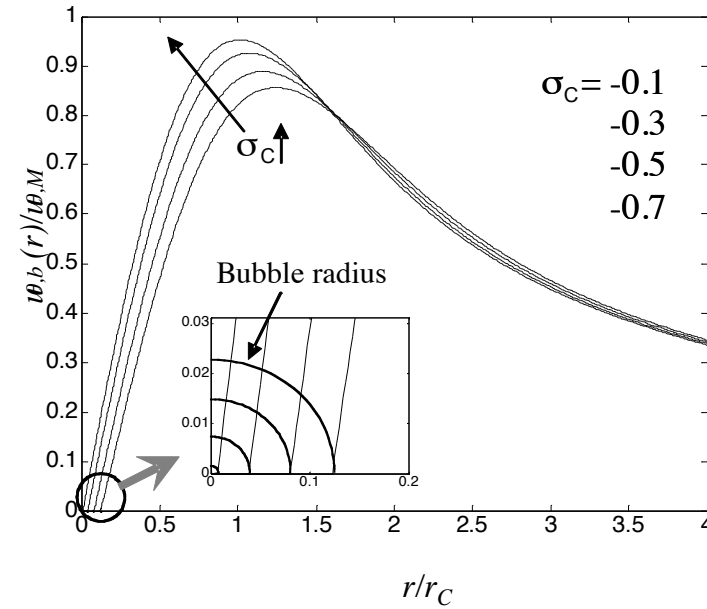
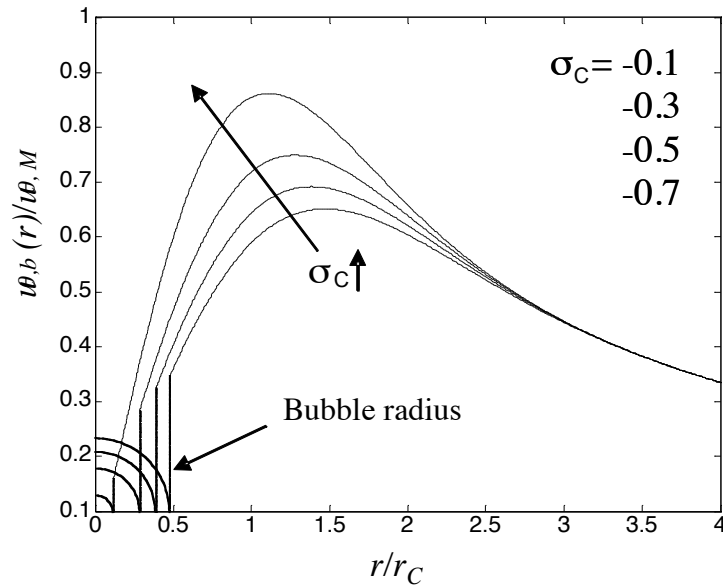
Near Spherical

Detectable noise is produced by **growth**, fission (infrequently), and **collapse**.

No "chirps" were detected

The acoustic impulse is **2 orders of magnitude less** than that produced by nearly spherical bubbles.

Size Scaling of 2-Dimensional Elongated Vortex Cavitation Bubble Radius



Maximum bubble angular velocity

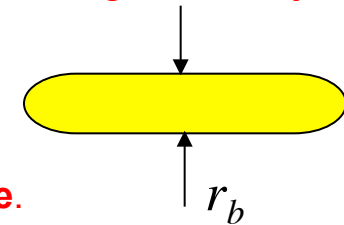
$\gamma = 0$

$\gamma = 1$

Minimum bubble angular velocity

Conserve angular momentum and kinetic energy
 Vapor pressure on the bubble surface
 Flow field is modified Gaussian.

γ is related to the tangential fluid velocity at the bubble interface.



Dynamics of Two-Dimensional and Axisymmetric Vortex Bubble Dynamics

Choi, Hsiao, Chahine, and Ceccio, *JFM*, (2009)

Continuity:

$$\frac{1}{r} \frac{\partial}{\partial r} (r \cdot u_r) = 0 \quad r_D > 1000 r_c$$

Momentum in r -direction:

$$\rho \left(\frac{\partial u_r}{\partial t} + u_r \frac{\partial u_r}{\partial r} - \frac{u_\theta^2}{r} \right) = -\frac{\partial P}{\partial r} + \mu \left(\frac{\partial^2 u_r}{\partial r^2} + \frac{1}{r} \frac{\partial u_r}{\partial r} + \frac{u_r}{r^2} \right)$$

Momentum in θ -direction:

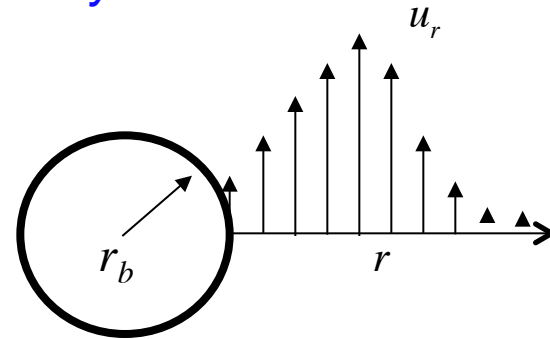
$$\rho \left(\frac{\partial u_\theta}{\partial t} + u_r \frac{\partial u_\theta}{\partial r} - \frac{u_r u_\theta}{r} \right) = \mu \left(\frac{\partial^2 u_\theta}{\partial r^2} + u_r \frac{\partial u_\theta}{\partial r} - \frac{u_\theta}{r^2} \right)$$

Boundary Conditions:

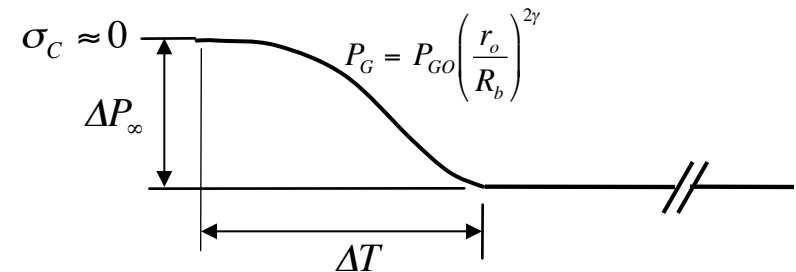
$$u_r|_{r=r_b} = \frac{dr_b}{dt} \quad P_{r=r_b} = P_V \quad P_\infty(t) \approx P_{1000r_c}(t)$$

$$\left. \frac{du_r}{dr} \right|_{r=r_b} \text{ not specified}$$

Cylindrical Bubble in an
Initially Gaussian Vortex



$$P_B = \frac{1}{\rho} \left(P_V + P_G - 2\mu \frac{\dot{R}_b}{R_b} - \frac{S}{R_b} \right)$$



Scaling of Two-Dimensional and Vortex Bubble Dynamics

r_C/r_O (core size / nucleus size)

$$r_C \gg r_O$$

r_C/r_D (core size / domain size)

$$r_D \gg r_C$$

Reynolds Number

$$\mathbf{Re}_\Gamma = \Gamma/\nu$$

Cavitation Number

$$\sigma_c = \frac{(P_{\infty 0} + \Delta P_{\infty}) - P_B}{\frac{1}{2}\rho \left(\beta \frac{\Gamma_O}{2\pi r_C} \right)^2} - \frac{2\eta}{\beta^2} = \frac{\Delta P_{\infty}}{\frac{1}{2}\rho \left(\beta \frac{\Gamma_O}{2\pi r_C} \right)^2}$$

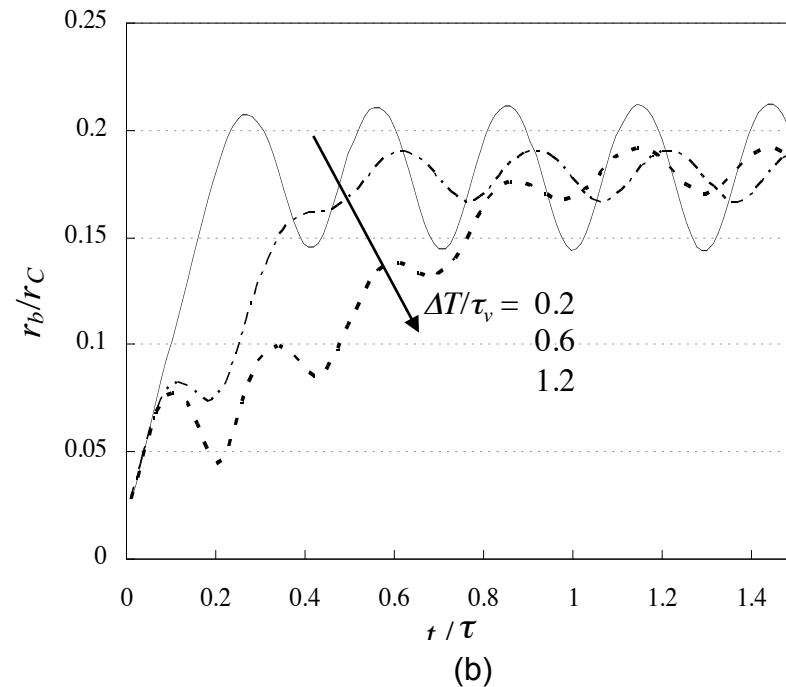
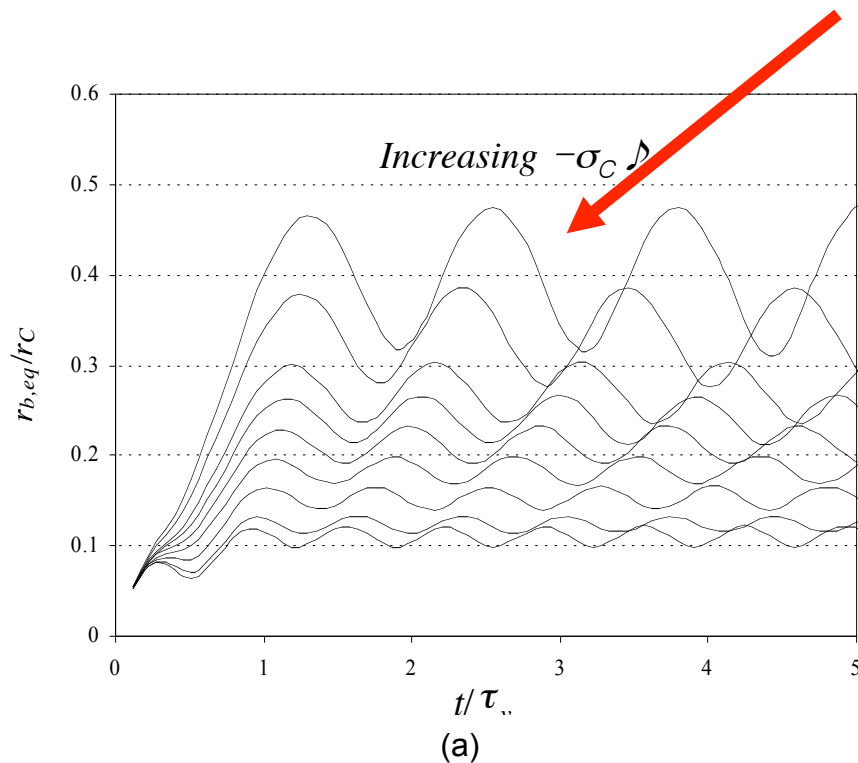
Externally Applied Tension

$$\frac{P_{\infty 0}}{\Delta P_{\infty}} = \frac{1}{\sigma_c} \left[\frac{\left(P_V - \frac{2S}{R_{bo}} \right)}{\frac{1}{2}\rho \left(\beta \frac{\Gamma_O}{2\pi r_c} \right)^2} + \frac{2\eta}{\beta^2} \right]$$

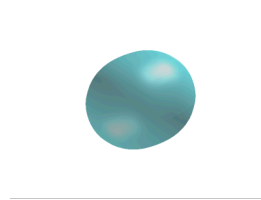
Time Scale

$$\frac{\Delta T}{\tau_v} = \Delta T \frac{\beta \Gamma_O}{4\pi^2 r_c^2}$$

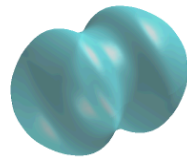
Vorticity Redistribution Leads To Dynamic Compliance



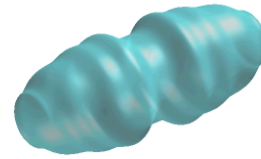
(a) Growth of the two-dimensional bubble as a function of time for $\Gamma_0 = 0.2$, $r_C = 4$ mm, with $\Delta T/\tau_v = 1.0$. The results for nine cavitation numbers are shown, $\sigma_C = 0.05, -0.1, -0.2, -0.4, -0.5, -0.6, -0.8, -1.0$; (b) Growth of the bubble for $\sigma_C = -0.3$, with $\Delta T/\tau_v = 0.25, 0.6$, and 1.2 .



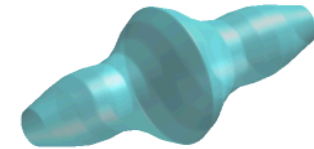
$t/\tau_v = 0.25$



$t/\tau_v = 0.5$

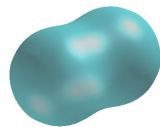


$t/\tau_v = 0.75$

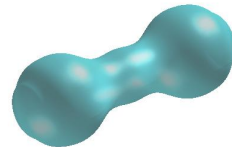


$t/\tau_v = 1$

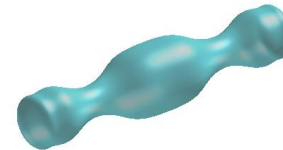
(a)



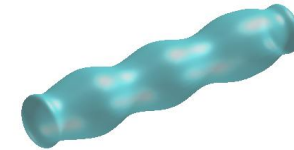
$t/\tau_v = 0.25$



$t/\tau_v = 0.38$

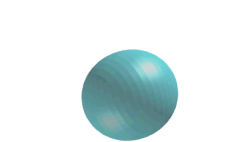


$t/\tau_v = 0.5$

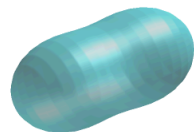


$t/\tau_v = 0.75$

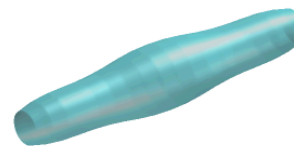
(b)



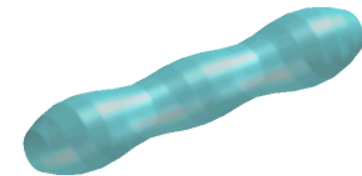
$t/\tau_v = 0.06$



$t/\tau_v = 0.19$



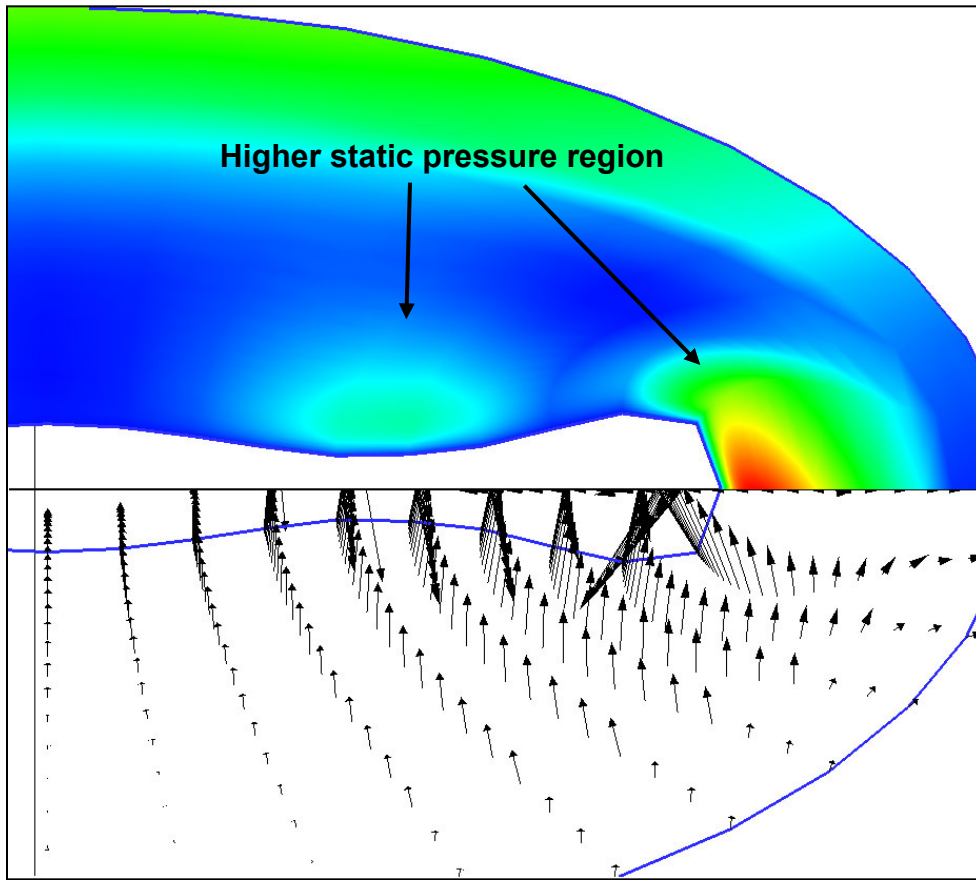
$t/\tau_v = 0.3$



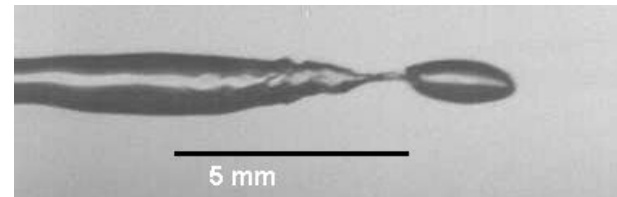
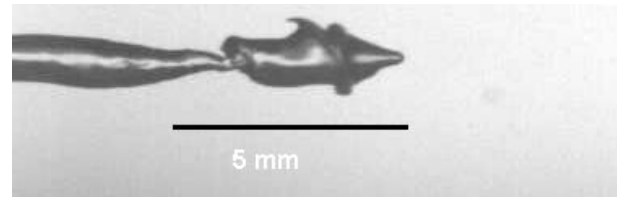
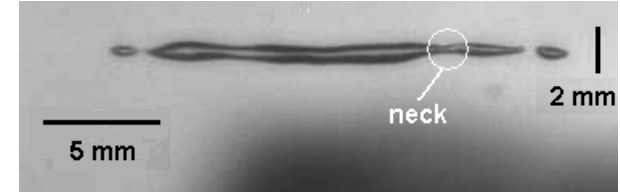
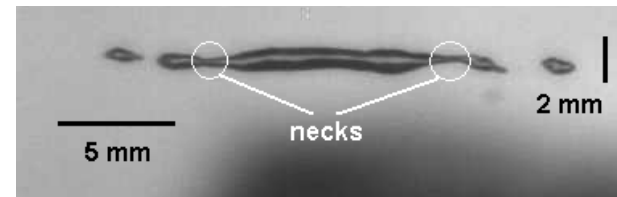
$t/\tau_v = 0.5$

(c)

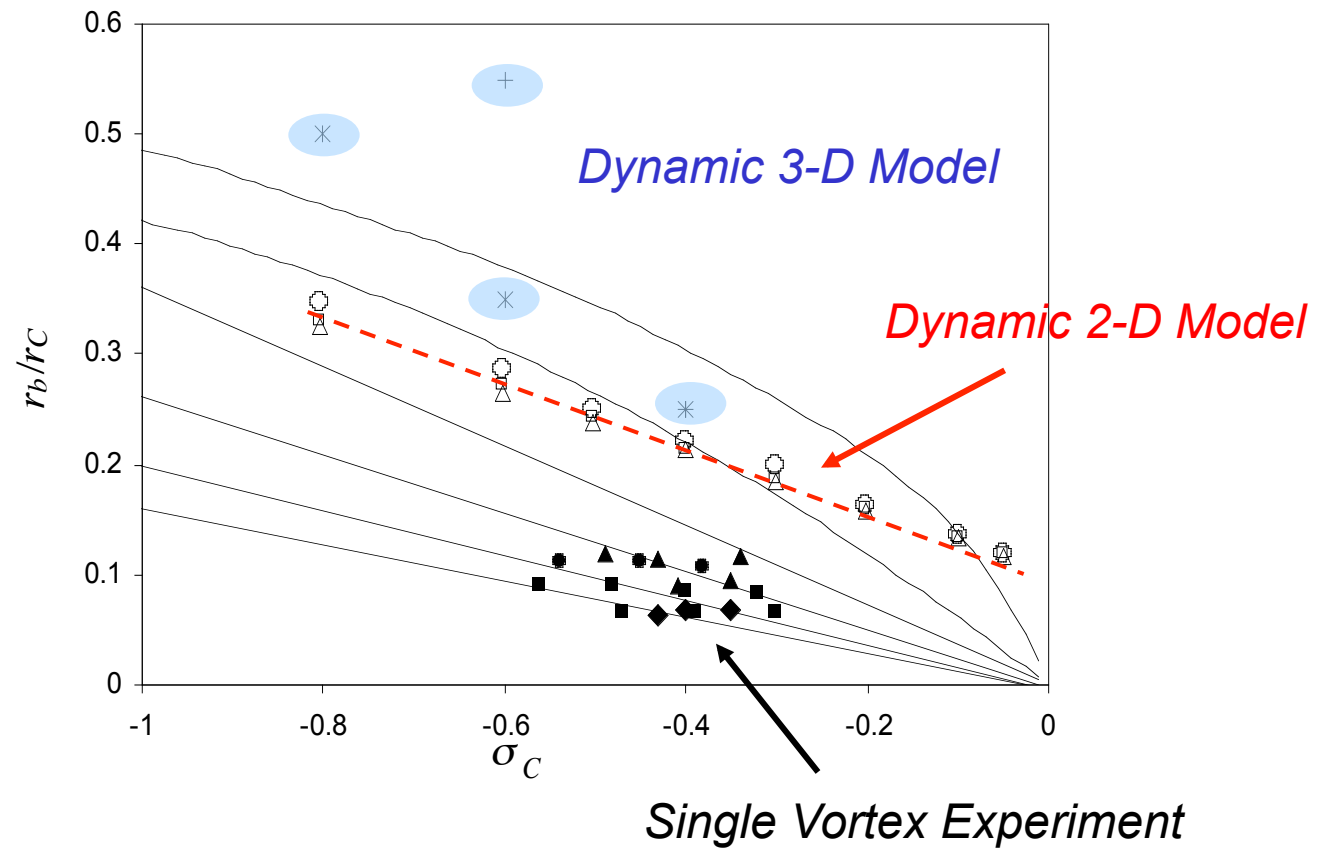
Volume history of three dimensional bubble geometry during growing for (a) $Re_F = 2 \times 10^5$ and $\sigma_C = -0.4$, for and $\Delta T/\tau_v = 0.46$ (b) $\Delta T/\tau_v = 1.13$. Also shown is the volume history for (c) $Re_F = 4 \times 10^5$ and, $\sigma_C = -0.4$, and $\Delta T/\tau_v = 0.23$.



$$\tau/\tau^* = 6, Re_T = 4 \times 10^5, L_b/D_b = 2 \text{ and } \sigma_C = 0.3$$



Comparison of the Predicted and Measured Radii of Elongated Vortex Bubbles



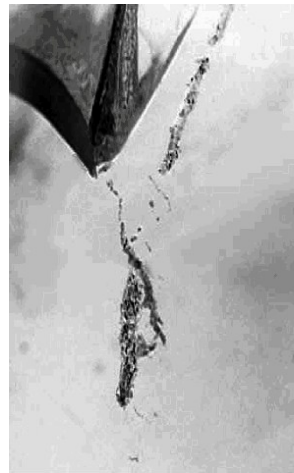
Summary Of Single Vortex Results

- Single vortex scaling methods will often not capture the physics responsible for TVC cavitation, especially when multiple interacting vortices are present.
- **There were no experimental observations of chirping bubbles in the single vortex experiment.**
- Analysis and numerical modeling suggest that chirping bubbles occur when there is a variation in angular momentum due to the change in the elongated bubble radius that couples into the pressure at the bubble interface.
- The analysis suggests that the rate of pressure changes surrounding the nucleus is important.

Summary Of Single Vortex Results

We therefore need to vary the rate of pressure reduction and recovery surrounding the bubble.

This can be achieved with vortex-vortex interactions.

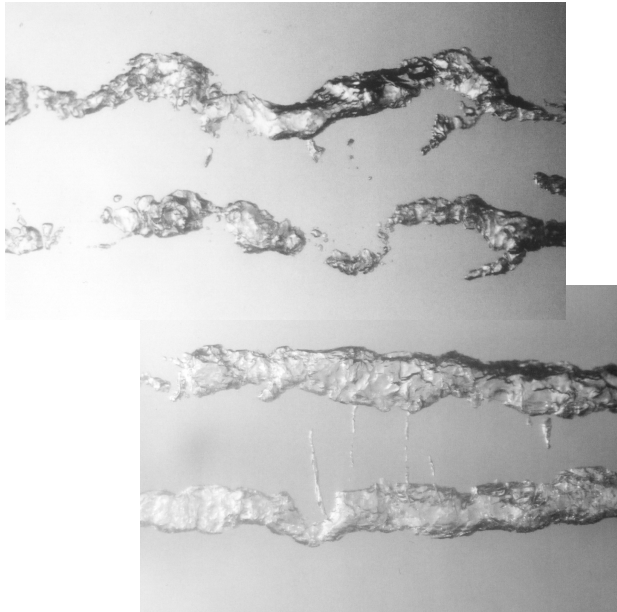


On cooperative instabilities of parallel vortex pairs

By R. L. BRISTOL, J. M. ORTEGA, P. S. MARCUS
AND Ö. SAVAŞ

Department of Mechanical Engineering, University of California at Berkeley,
Berkeley, CA 94720-1740, USA
savas@me.berkeley.edu

(Received 11 February 2003 and in revised form 24 June 2004)



**UM Visualizations of cavitating
co-rotating vortices.**

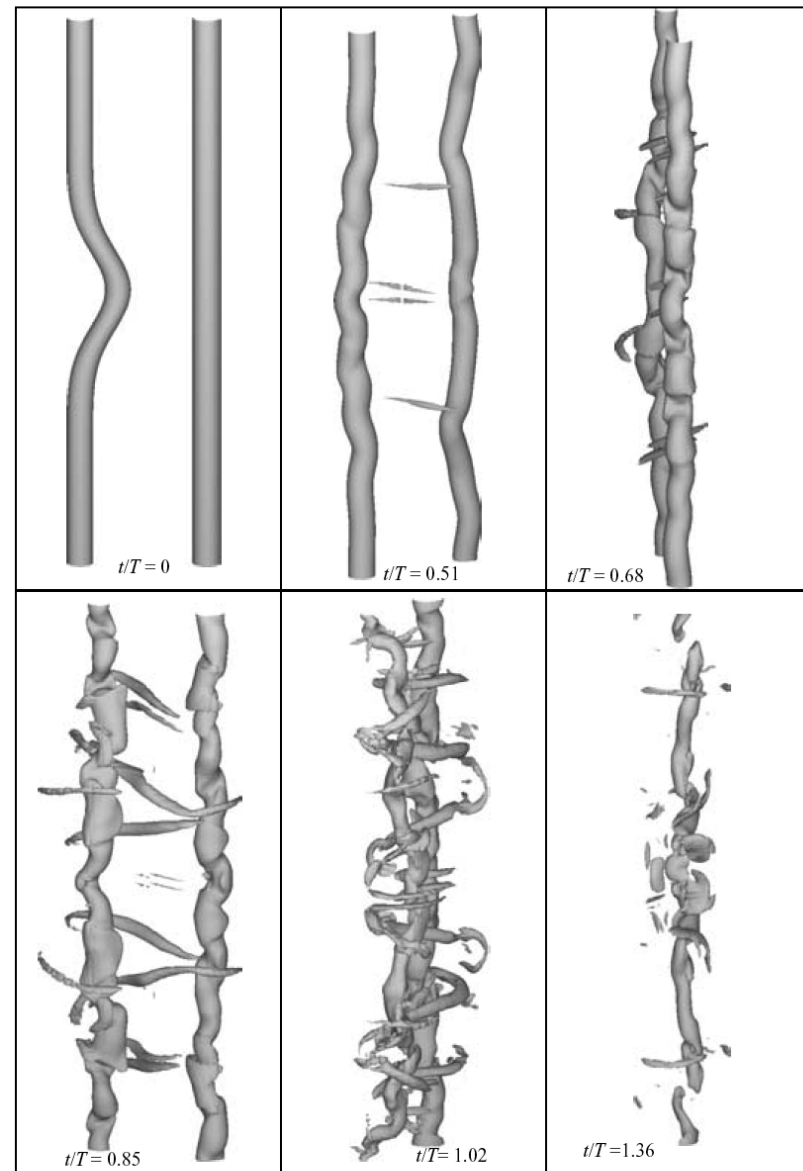


FIGURE 14. Simulation of a $(\Gamma, d/\sigma) = (0.9, 6.67)$ co-rotating pair perturbed by a hump of amplitude 2σ on the weaker vortex. Some indication of elliptic instability is visible at $t/T = 0.68$ (compare to $t/T = 0.61$ in figure 12). Vorticity bridges become clearly visible at $t/T = 0.85$. Orbital period $T = 147$ s.

UM Visualizations of cavitating counter-rotating vortices.

On cooperative instabilities of parallel vortex pairs

353

Secondary Vortex

Primary Vortex

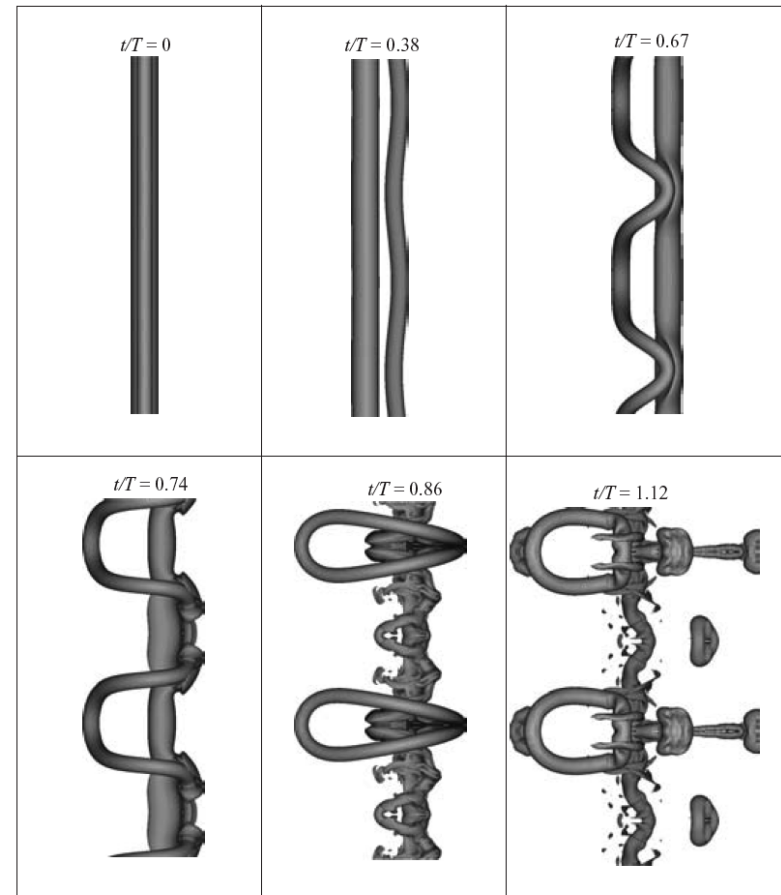
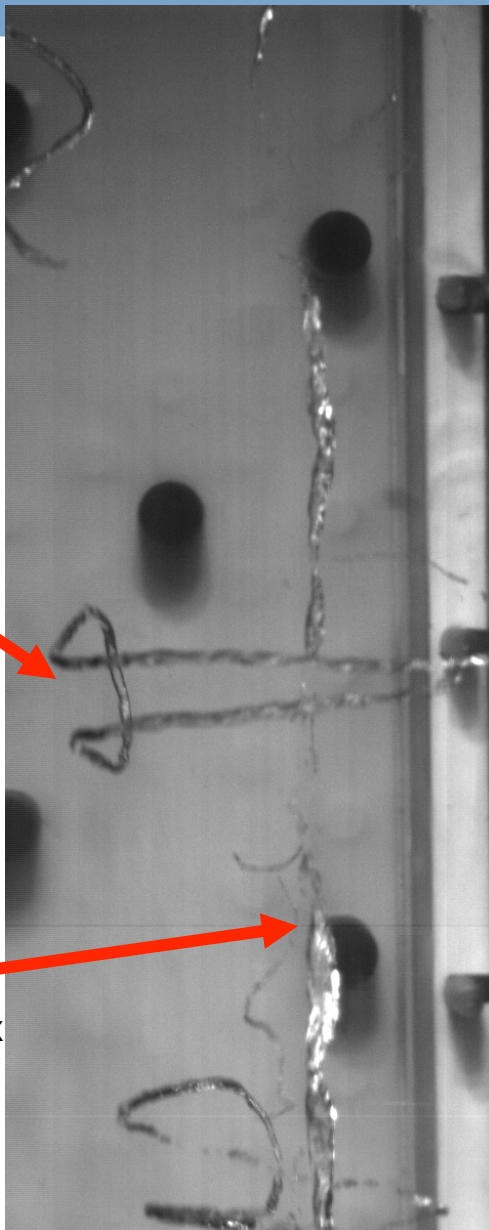
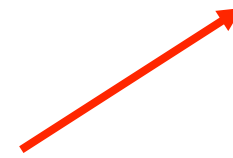


FIGURE 15. Surfaces of a $\Gamma = -0.37$, $d/\sigma_1 = 3.96$, $d/\sigma_2 = 7.47$ counter-rotating pair. The weaker vortex is perturbed at $(kd)_{max}$ at $t=0$. View is edge-on at $t=0$, with the weaker vortex in the foreground, and remains fixed throughout the simulation. Orbital period $T = 156$ s.

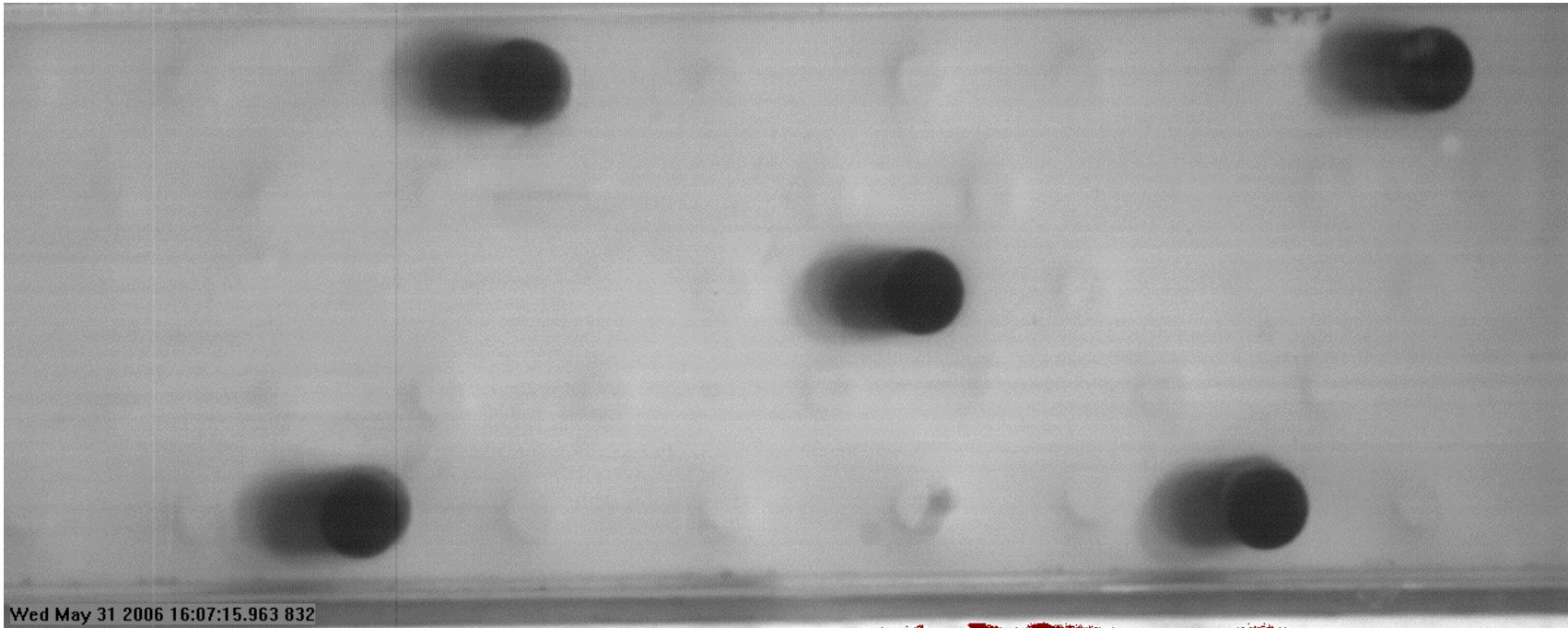
Counter-Rotating Vortex Pairs Examined

run#	$\Gamma_{OP}, m^2/S$	$\Gamma_{OS}, m^2/S$	r_{CP}, mm	r_{CS}, mm	Γ_{OS}/Γ_{OP}	b, mm	$(r_{CS}+r_{CP})/(2b)$	$Re \Gamma_P$	C_{PCP}	C_{PCS}	Ratio	Incepting Vortex	Instability
T1	0.252	-	4.76	-	-	-	-	252000	-1.24	-	-	-	-
T2	0.288	-	5.15	-	-	-	-	288000	-1.38	-	-	-	-
R1	0.257	-	3.75	-	-	-	-	257000	-2.07	-	-	-	-
R2	0.288	-	4.2	-	-	-	-	288000	-2.07	-	-	-	-
D1	-0.2915	0.0617	5.6	2.9	-0.21	23	0.185	291500	-1.19	-0.20	6.0	Primary	O
D2	-0.2916	0.0633	5.9	3.3	-0.22	21	0.219	291600	-1.08	-0.16	6.6	Simultaneous	O
D3	-0.2283	0.051	5.1	2.7	-0.22	22	0.177	228300	-0.88	-0.16	5.6	Primary	O
D4	-0.2976	0.0686	5.7	3.4	-0.23	21	0.217	297600	-1.20	-0.18	6.7	Secondary	O
D5	-0.2745	0.0662	5.3	2.7	-0.24	22	0.182	274500	-1.18	-0.26	4.5	Secondary	O
D6	-0.2266	0.0579	6	3.7	-0.26	21	0.231	226600	-0.63	-0.11	5.8	Secondary	O
D7	-0.2708	0.0798	6.2	3.7	-0.29	22	0.225	270800	-0.84	-0.21	4.1	Secondary	O
D8	-0.2226	0.0683	5.2	3.2	-0.31	22	0.191	222600	-0.81	-0.20	4.0	Primary	O
D9	-0.2621	0.0885	5.2	3	-0.34	21	0.195	262100	-1.12	-0.38	2.9	Secondary	O
D10	-0.2184	0.081	4.9	3	-0.37	21	0.188	218400	-0.88	-0.32	2.7	Primary	O
D11	-0.2671	0.1062	6.1	4.1	-0.40	21	0.243	267100	-0.85	-0.30	2.9	Secondary	O
D12	0.1106	-0.0519	4.3	3.3	-0.47	18	0.211	110600	-0.29	-0.11	2.7	Primary	X
D13	0.1439	-0.08	3.5	3.7	-0.56	19	0.189	143900	-0.75	-0.21	3.6	Primary	X
D14	0.1627	-0.096	4	3.5	-0.59	20	0.188	162700	-0.73	-0.33	2.2	Primary	X
D15	0.1849	-0.112	4.3	3.9	-0.61	19	0.216	184900	-0.81	-0.36	2.2	Primary	X
D16	0.1697	-0.1267	4	3.7	-0.75	20	0.193	169700	-0.79	-0.52	1.5	Secondary	O
D17	0.1638	-0.1236	3.9	3.6	-0.75	20	0.188	163800	-0.78	-0.52	1.5	Secondary	O

**Some combinations are unstable,
and the weaker secondary vortex cavitates first**



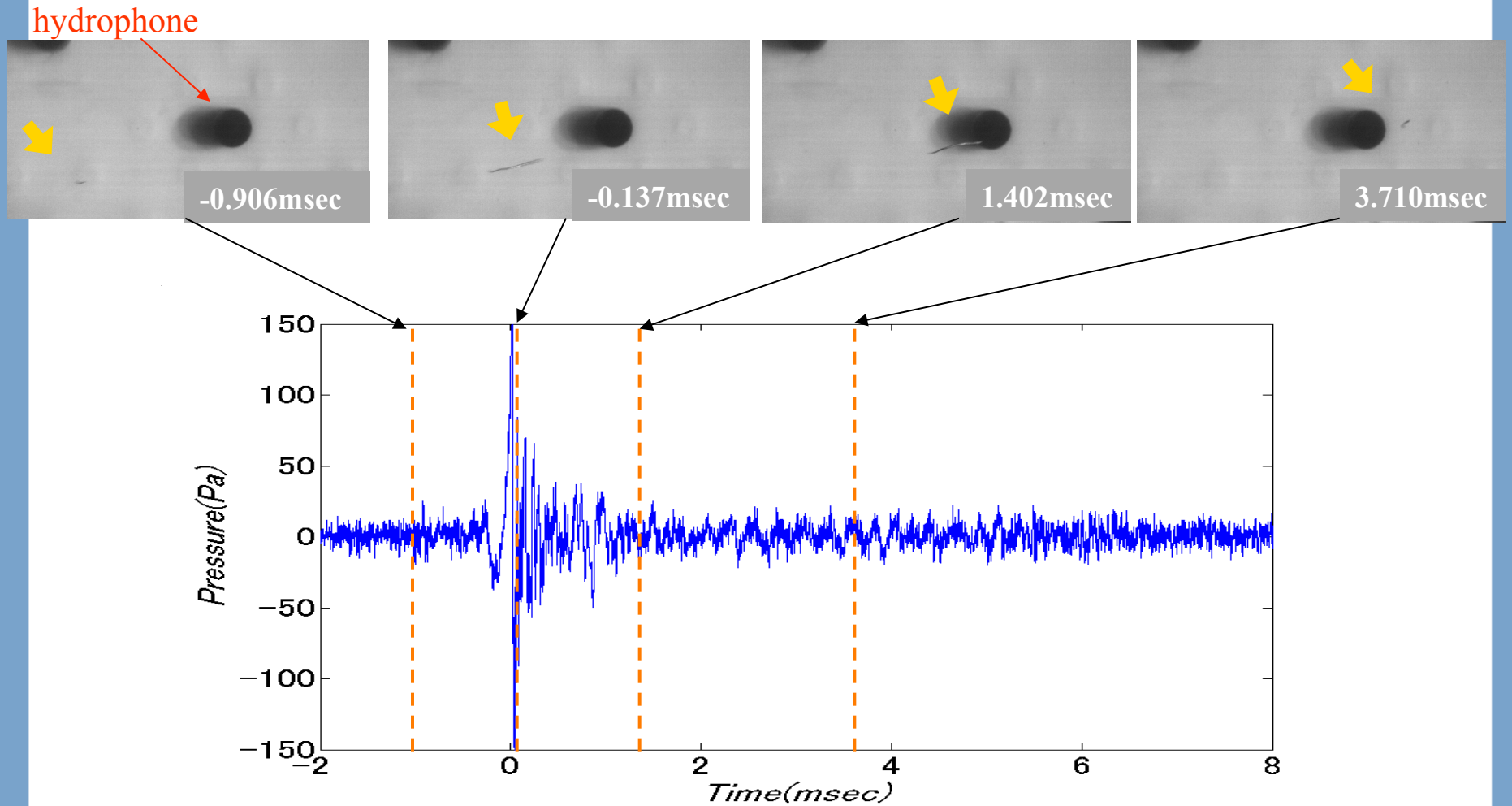
Vortex Inception in the Secondary Vortex



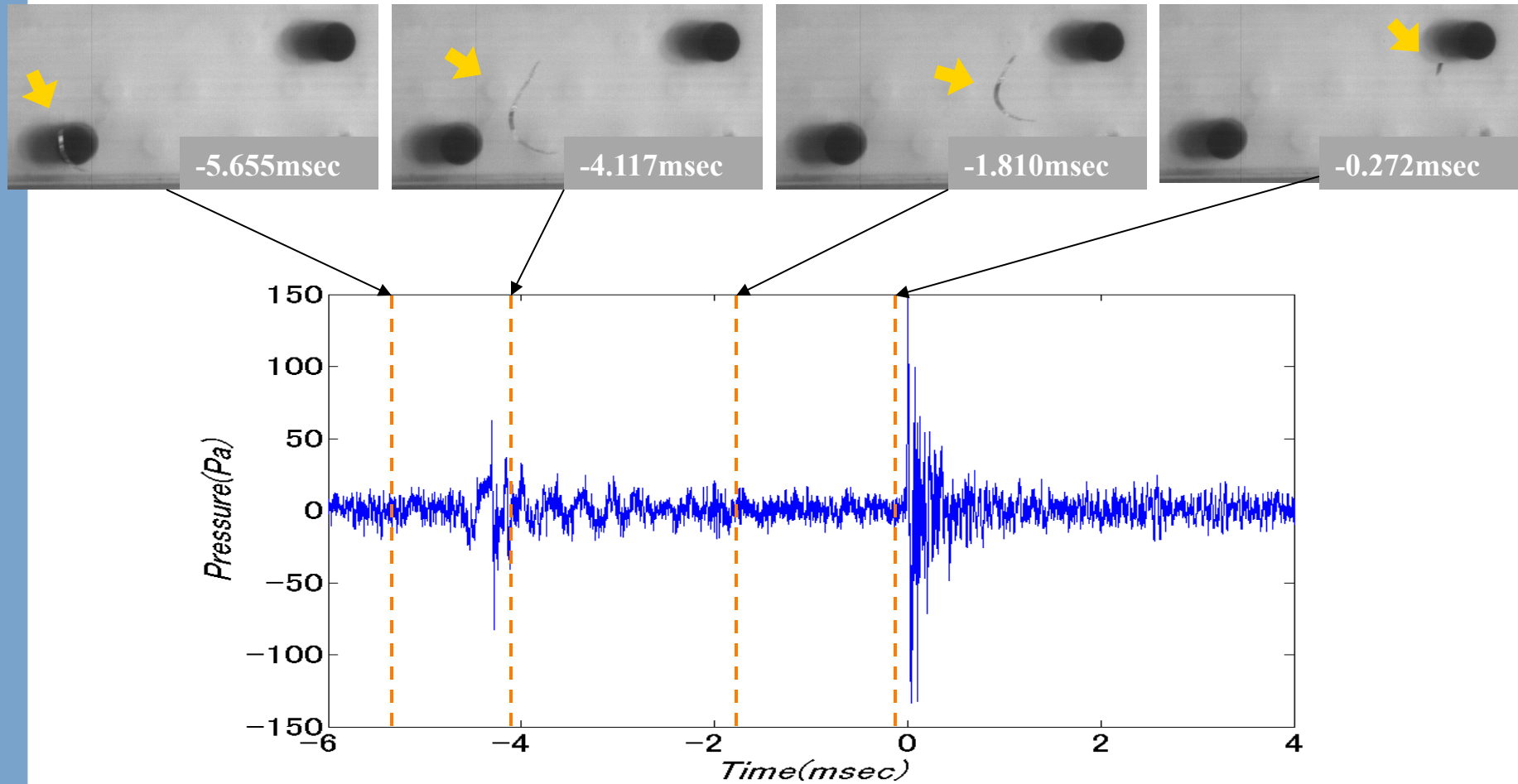
152 mm x 61 mm

2600 FPS

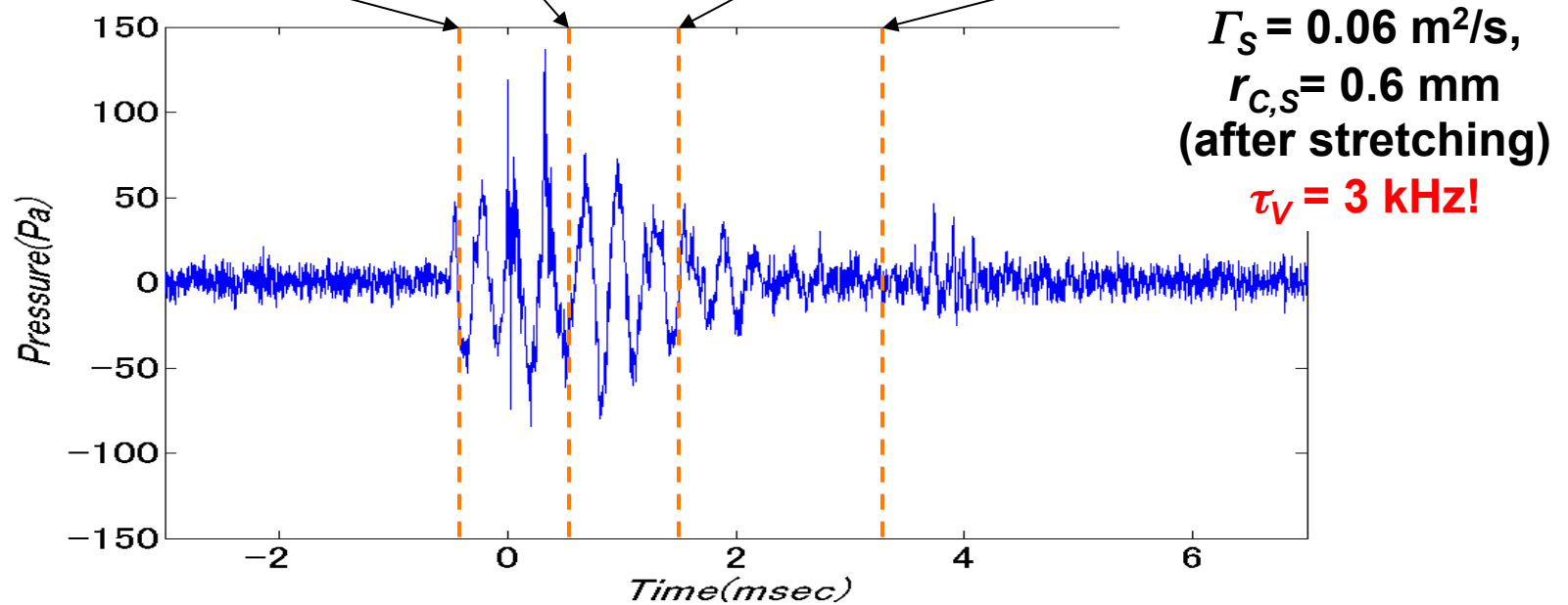
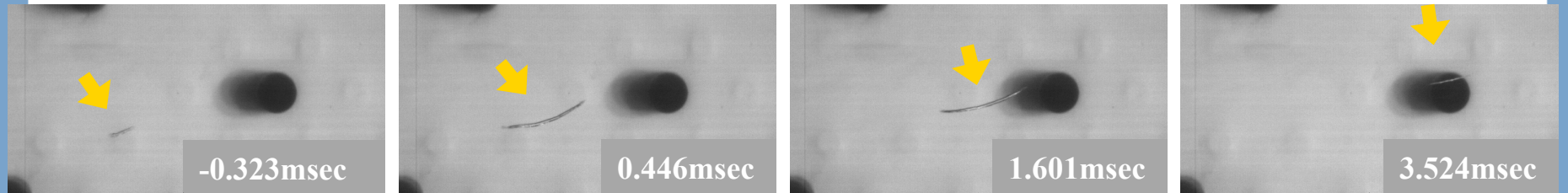
Growing Case Makes a "Pop"



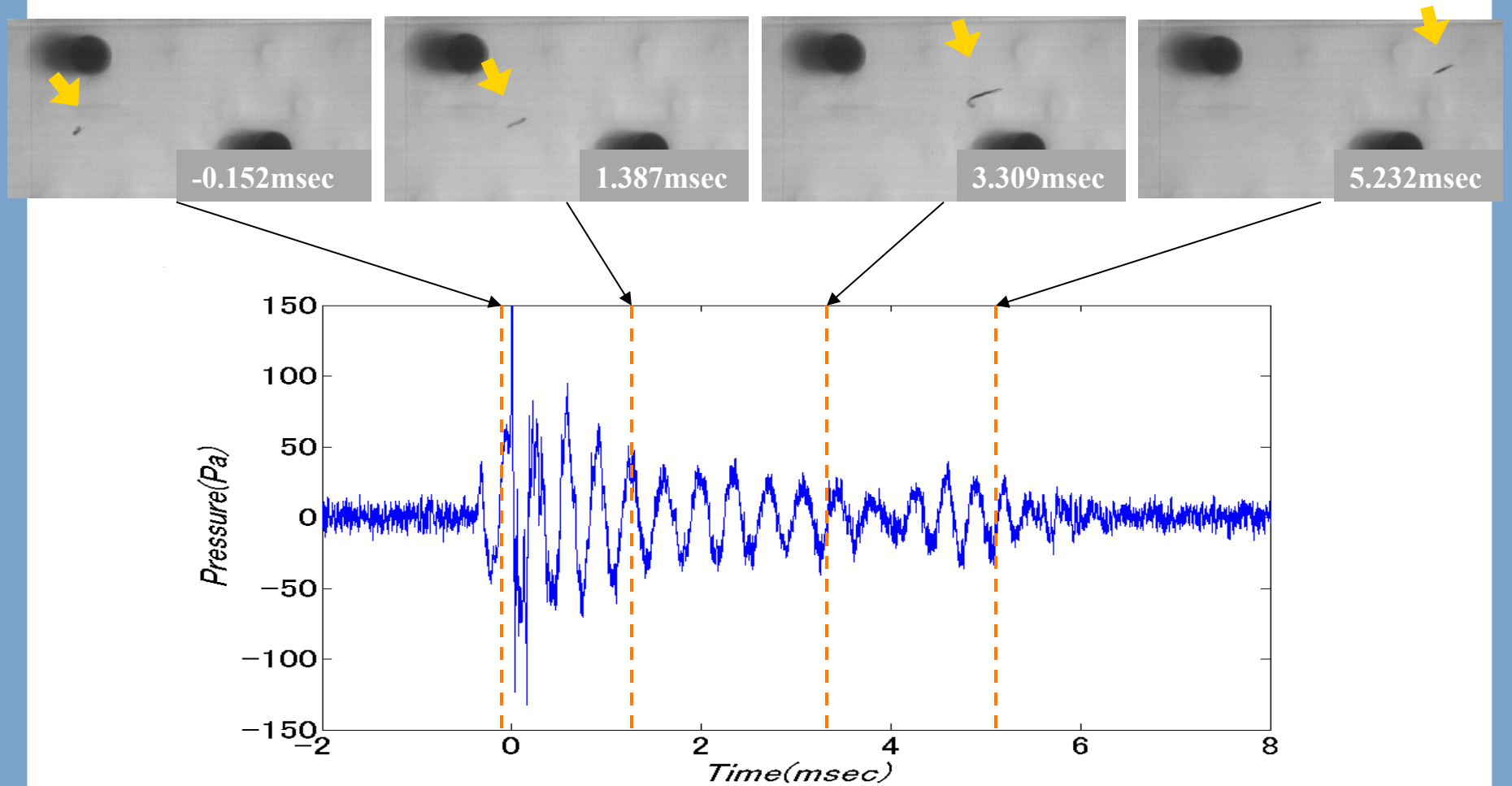
Collapsing Case Makes a “Pop”



“Chirping” After Inception



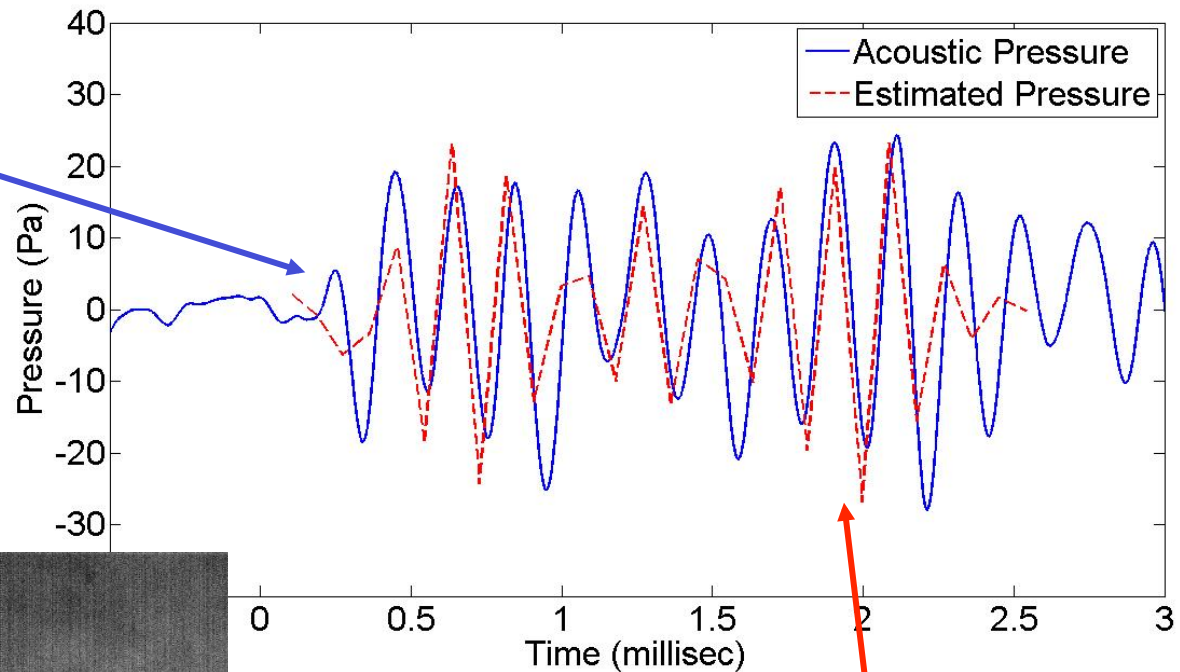
“Chirping” After Inception



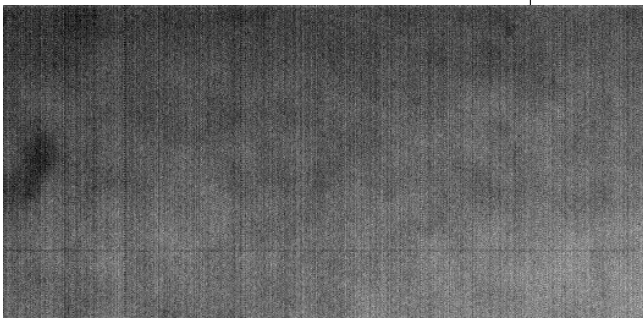
Acoustic Pressure: Inferred and Measured

Acoustic Pressure

$$P_{est} \approx \frac{\rho_w}{4\pi R} \frac{\partial^2 Q}{\partial t^2}$$

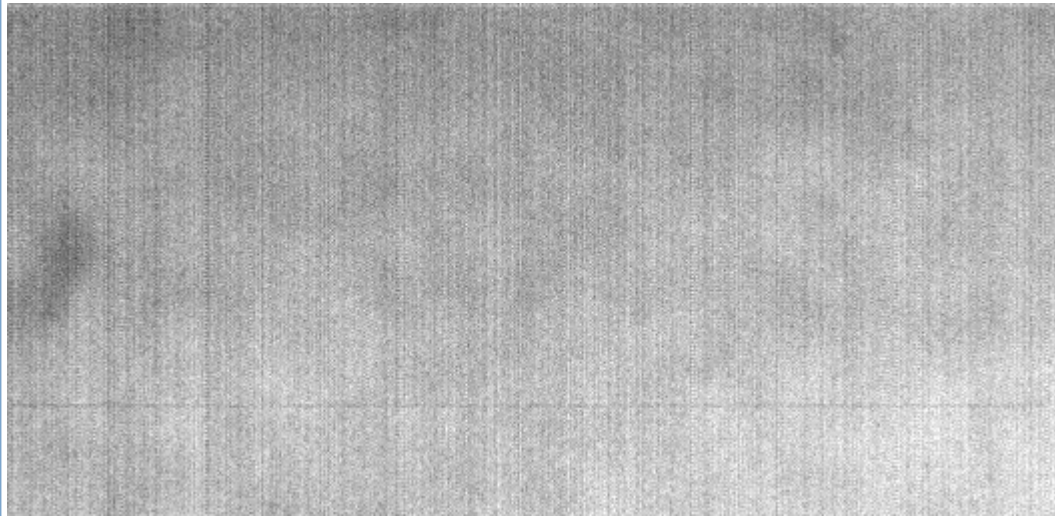


1 cm



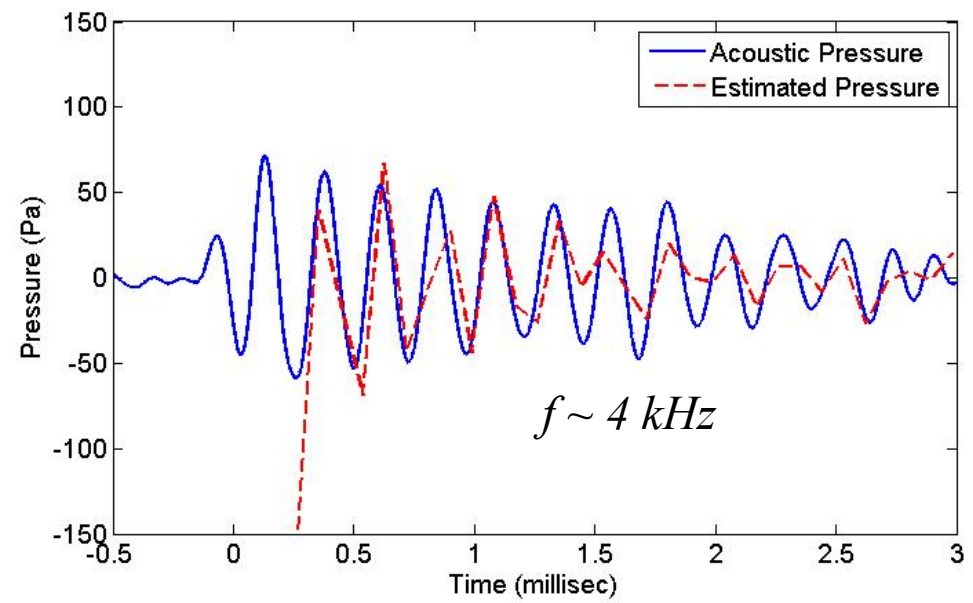
$P = 170\text{kPa}$
 $DO = 25\%$
 $\sigma_{\infty} = 3.3$

**Acoustic Pressure Computed
From Measured Volume
Acceleration**

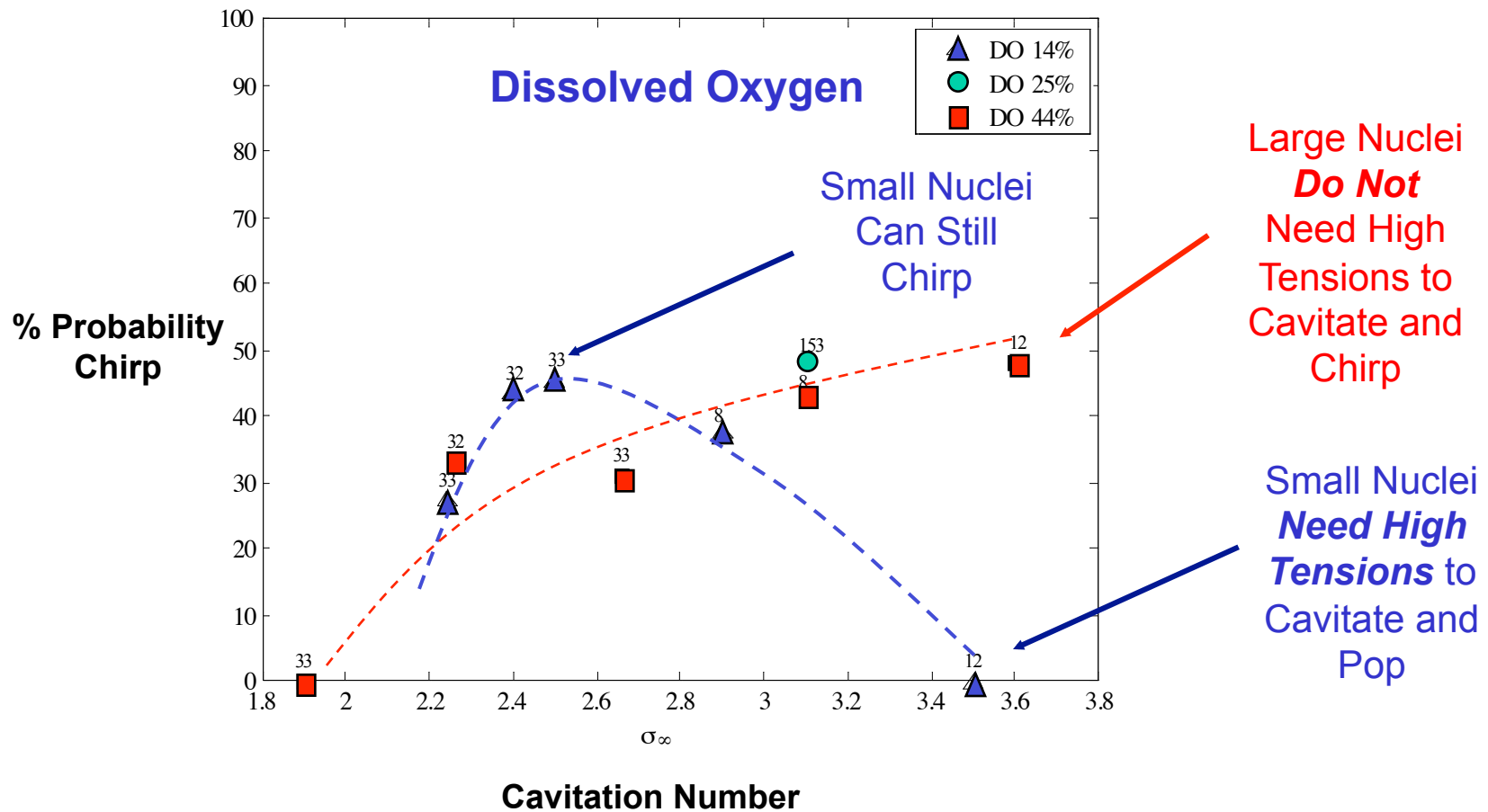


1 cm

$P = 170\text{kPa}$
 $DO = 25\%$
 $\sigma_{\infty} = 3.3$



Probability of a Chirp Is Related to Nuclei Size



Some Conclusions About TVC Inception and Acoustics

- Single vortex scaling methods will often not capture the physics responsible for TVC cavitation, especially when multiple interacting vortices are present.
- **Bubble-Vortex Interactions are important for understanding the dynamics and noise emissions of elongated vortex bubbles.**
- *A combination of experimental, analytical, and numerical tools are available to understand and (possibly) predict TVC cavitation since there is likely no single scaling method which captures all the necessary physics.*
- *The bubble could be used as a flow diagnostic (!)*

Some Acknowledgements

Dr. Stuart Jessup (NSWC-CD)
Dr. David Fry (NSWC-CD)
Dr. Chris Chesnakas (NSWC-CD)

Dr. Michael Billet (PSU-ARL)
Mr. William Straka (PSU-ARL)

Dr. George Chahine (Dynaflow)
Dr. Hsiao (Dynaflow)

Dr. Ki-Han Kim (ONR)

Prof. David R. Dowling (UM)
Prof. Ghanem Oweis (AUB)
Dr. Natasha Chang (NSWC-CD)
Dr. Jaehyung Choi



Prof. Roger Arndt



Prof. Chris Brennen

Thank you!